Development of L-bent Positron Detectors for μSR Applications at China Spallation Neutron Source

Ziwen Pan, Jingyu Dong, Zebin Lin, Zhe Wang, Jiandang Liu, Hongjun Zhang, Hao Liang, Bangjiao Ye, Hantao Jing, Jingyu Tang, Ye Yuan, Fang Xie, Daniel E. Pooley and Stephen P. Cottrell

***Abstract*—A 128-channel positron detection system will be constructed at Experimental Muon Source (EMuS) of China Spallation Neutron Source (CSNS) to conduct muon spin rotation/relaxation/resonance (μSR) measurements. Each detector channel consists of a scintillator, a light guide and a photomultiplier tube (PMT). The long light guide is bent to an "L" shape to propagate optical photons from the scintillator to the PMT. A series of Geant4 simulations and experiments have been done to optimize the light collection performance of the L-bent detector. Geometry deformation induced by the bending process has been well modelled. Simulation results agree with the experimental tests. Accordingly, a novel hybrid wrapping method (scintillator with polytetrafluoroethylene (PTFE), light guide with aluminum tape) has been developed to improve the amplitude of detector signals greatly. Compared to wrapping the detector with merely PTFE tapes or aluminum tapes, this method leads to an enhancement in light collection efficiency of 73% or 14%, respectively. Two optimally manufactured prototype detectors using the novel wrapping method have been tested at the ISIS Muon Facility. The beam tests demonstrated that the L-bent detectors can precisely measure the behavior of muon spins inside samples. Therefore, the L-bent detector design is competent for μSR applications at CSNS/EMuS.**

***Index Terms*—L-bent positron detector, light collection performance, Geant4 simulation, hybrid wrapping method, μSR**

I. INTRODUCTION

MUON spin rotation, relaxation and resonance (μSR) spectroscopy uses highly polarized ($\sim$ 100%) muons to probe properties of condensed matter concerning magnetism [1], superconductivity [2] and molecular dynamics [3] at a microscopic level [4]. Polarized muons can do Larmor precessions in the internal magnetic field inside a sample, and decay into positrons asymmetrically with a lifetime of $\sim$ 2.2 μs. The angular distribution of positrons depends on the interactions between the muon spin and its magnetic field surrounding. Detecting the asymmetry by arranging detector arrays in the forward and backward directions with respect to the sample can help us reveal the magnetic structure and relevant properties of materials.

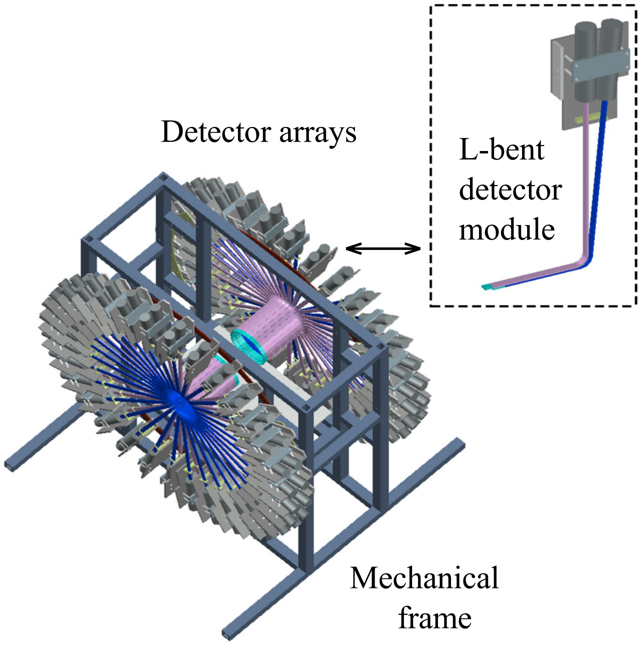

Fig. 1. Detector arrangement of the 128-channel μSR spectrometer prototype with 64 detector modules in both forward and backward direction of the sample. Each detector module consists of a scintillator (small cyan block), an L-bent light guide, and a photomultiplier tube (PMT, gray tube). Two detector modules are stacked together.

The pulsed Experimental Muon Source (EMuS) has been proposed to be built at China Spallation Neutron Source (CSNS) using 5% (5 kW, 2.5 Hz) of its proton beam power (100 kW, 1.6 GeV, 25 Hz) [5]. A 128-channel positron detection system is under construction to prototype a μSR spectrometer for EMuS, and has the potential to be extended into several hundred channels. The μSR spectrometer prototype has 2 rings in both forward and backward banks relative to the sample as shown in Fig. 1. And each ring consists of 32 detectors. The sizes of scintillators are 20 mm $\times$ 19.5 mm $\times$ 5 mm for outer rings, and 31 mm $\times$ 18.5 mm $\times$ 5 mm for inner rings. The light guide is 750 mm in length, and it is bent with an "L" shape at its quarter. For typical μSR applications, external fields up to several thousand Gauss [6] or several Tesla [7], [8] are required. Under such conditions, there are two scenarios

---

This work was supported by the National Natural Science Foundation of China (Grant No. 12005221, 11527811), and the State Key Laboratory of Particle Detection and Electronics (SKLPDE-ZZ-202018) at University of Science and Technology of China. (*Corresponding author: Ziwen Pan, Bangjiao Ye.*)

Ziwen Pan, Jingyu Dong, Zebin Lin, Zhe Wang, Jiandang Liu, Hongjun Zhang, Hao Liang and Bangjiao Ye are with the State Key Laboratory of Particle Detection and Electronics, University of Science and Technology of China, Hefei, 230026, China (e-mail: panzw19@ustc.edu.cn, bjye@ustc.edu.cn).

Hantao Jing and Jingyu Tang are with the Institute of High Energy Physics, Chinese Academy of Sciences (CAS), Beijing 100049, China, and also with the Spallation Neutron Source Science Center (SNSSC), Dongguan 523803, China.

Ye Yuan is with the Institute of High Energy Physics, Chinese Academy of Sciences (CAS), Beijing 100049, China.

Fang Xie is with the Department of Physics and Astronomy, University College London, London, WC1E 6BT, U.K.

Daniel E. Pooley and Stephen P. Cottrell are with the ISIS Facility, STFC Rutherford Appleton Laboratory, Chilton, Oxfordshire OX11 0QX, U.K.

This article has been accepted for publication in a future issue of this journal, but has not been fully edited. Content may change prior to final publication. Citation information: DOI 10.1109/TNS.2021.3099685, IEEE Transactions on Nuclear Science

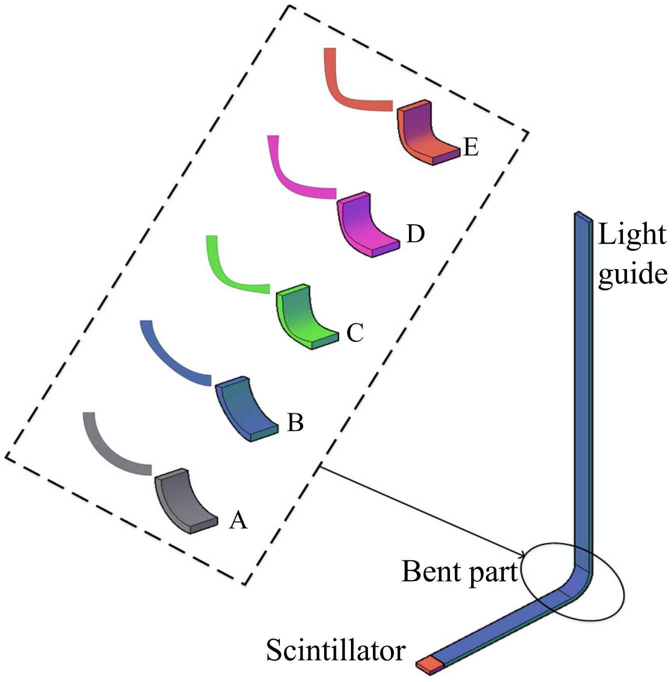

Fig. 2. Geometry construction of the positron detector in Geant4. The bent part is modelled with five shapes using the loft method in AutoCAD: (A) perfect quarter tube, (B) draft angle, (C) normal to end sections, (D) normal to start sections, (E) normal to all sections.

available for μSR detector design: 1) scintillator + light guide / optical fiber + PMT [6], [7], [9], [10], 2) scintillator + (optical fiber) + Silicon photomultiplier (SiPM) [8], [11]–[13]. As PMTs have relatively short deadtime compared with SiPMs according to their usage at muon facilities, the former scenario has been selected to accept the intense muon pulses at CSNS/EMuS. Novel Device Laboratory [14] and Sensl [15] have developed types of SiPMs with short recovery times (∼10 ns). It is promising for developing highly segmented μSR spectrometers with several thousand channels at EMuS in the future.

To avoid the decrease of PMT output amplitudes due to the high magnetic field in the sample area, the PMTs are mounted outside the magnetic coils. The L-bent light guides are used to transport photons from the scintillator to the PMTs. These light guides were hand-bent after short-time heating, resulting in shape-deformations in the bent parts. The usage of a long L-bent light guide and inevitable bending deformations will reduce the amplitude of detector signals, which can affect the quality of μSR data. The combination of plastic scintillators and light guides has been successfully applied in μSR spectrometers like MUSR/EMU/HiFi at ISIS [6], [7] and DΩ1 at J-PARC [10]. Particularly, light guides are bent to different shapes among three spectrometers at ISIS. However, there is seldom information focusing on the influences of wrapping methods and surface treatments for both scintillator and light guide, and geometry deformations induced by the bending process on the amplitudes of output signals. These influences are crucial in the discrimination of background events, detector noise and low energy positrons which occupy low asymmetries in μSR measurements. Therefore, we have taken a further investigation focusing on the impacts of wrapping methods, surface treatments, and geometry deformations on the light collection. A series of Monte Carlo simulations and experimental tests have been done to quantify these influencing factors and optimize the light collection performance. The experimental tests consist of lab-tests in the domestic laboratory and beam tests at ISIS Muon Facility [16]. Both tests demonstrated that the L-bent positron detectors satisfy the requirements of μSR applications at CSNS/EMuS.

TABLE I
OPTICAL PROPERTIES OF THE SCINTILLATOR, LIGHT GUIDE AND WRAPPING MATERIALS SET IN GEANT4.

EJ200 scintillator [22]	Refractive index Light yield (photons/MeV) Emission peak (nm) Absorption length (cm) Rise time (ns) Decay time (ns)	1.58 10000 425 380 0.9 2.1
Light guide (PMMA)	Refractive index Absorption length (cm)	1.489 350
PTFE tape	Reflection mode Finish Reflectivity	Diffusive groundbackpainted 0.934 [23]
Aluminum tape	Reflection mode Finish Reflectivity	Specular polishedbackpainted 0.944 [23]

II. SIMULATION MODEL

Geant4 [17]–[19] is a powerful Monte Carlo simulation toolkit in the design of particle detectors. It provides abundant physical processes and particles for users to fit the toolkit into their specific situations. As the gamma energy induced by sodium-22 (^{22}Na) is in the same range of positron energy deposition in plastic scintillators, it is chosen to calibrate the light collection performance of the positron detector. To exactly simulate such experimental configuration, the radioactive decay model, the standard electromagnetic model including photoelectric effect, Compton scattering and positron-electron annihilation, and the optical processes dedicated to optical photons are fully considered in the simulation model.

A. Definition of detector geometries

Detectors with regular shapes (box, tube, sphere, etc.) can be directly modelled by implementing the Constructive Solid Geometry (CSG) representations in Geant4. The toolkit permits Boolean operations on several CSG solids to build special geometries. Besides these standard methods, an auxiliary toolkit named “CADMesh” [20] can import CAD models into Geant4. The hand-bending process in the production of L-bent detectors causes random deformations which cannot be easily modelled in Geant4. To understand the influences of bending deformations on the light collection efficiency (LCE), the bent part was modelled in AutoCAD (educational version) using the loft command. Fig. 2 shows one perfect and four distorted geometries drawn by AutoCAD and read by Geant4. Among four distorted shapes, shapes B and E have a thinner part in the middle, and shapes C and D have such part in the bottom

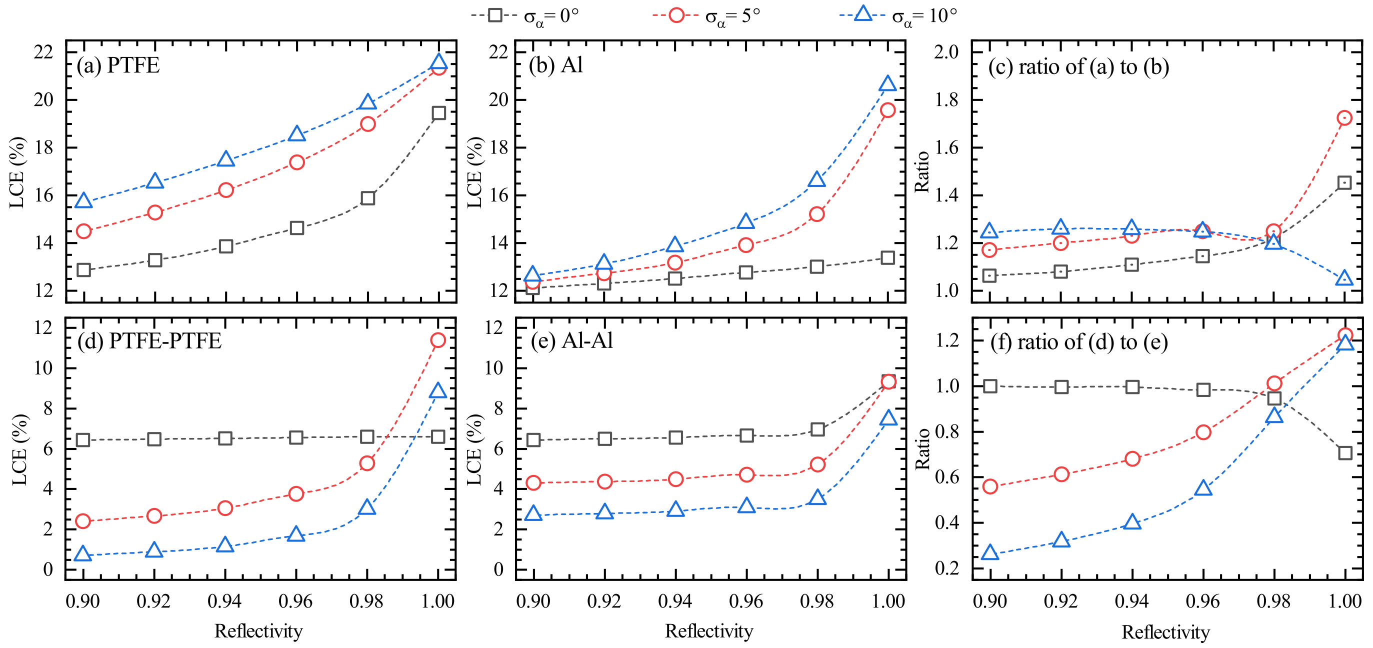

Fig. 3. The light collection efficiency of (a, b) a scintillator and (d, e) a long straight detector (scintillator + long straight light guide) with different wrapping materials, and (c, f) their ratios. The first wrapping material is for the scintillator, and the second is for the light guide in both (d, e). The uncertainties are within 1% of the data points, which are too little to be displayed.

and upper positions, respectively. Note that, the perfect shape can be directly constructed in Geant4. The dimension of the scintillator is 20 mm × 22 mm × 5 mm, and the light guide is 22 mm × 5 mm with an L-bent shape at its quarter position for all investigation simulations and experiments. The geometry of such detector is similar to the real positron detectors tested at ISIS Muon Facility. Therefore, the optimization of its light collection performance is applicable for the real detectors.

B. Optical processes of photons inside the detector

For a scintillation detector, the energy deposition of ^{22}Na is definite once its geometry and material are fixed. However, the transport of optical photons generated by the energy deposition can be affected by the geometry, material and surface treatment of the detector. A good configuration of all these factors can help optimize the detector performance which is determined by the number of detected optical photons. In Geant4, relevant processes regarding the generation and propagation of optical photons are G4Scintillation, G4OpAbsorption and G4OpBoundaryProcess. The former two processes depend on the intrinsic optical properties of detector materials. The last one manages the reflection behavior of optical photons when hitting the surface boundary. The UNIFIED model in G4OpBoundaryProcess is chosen to simulate the influence of wrapping materials treated as surface boundaries. In this model, the dielectric or metallic property, finish treatment, reflectivity, reflection mode, and quantum efficiency (QE) of the photocathode in a PMT should be assigned to all surfaces where optical photons may hit [21].

Table I lists the main properties of the scintillator, light guide and wrapping materials for the production of positron detectors. In Geant4, the finish of the diffusive or specular surface is set as ground or polished, respectively. The item "backpainted" in the surface finish setup means an air gap between a crystal (transparent object) and its wrapper. In this kind of surface, optical photons hit the crystal-air gap interface at first. If reflection happens, one of the four reflection modes (specular spike, specular lobe, backscatter and Lambertian) takes place according to assigned roughness. If refraction happens, the optical photon will hit the air gap-wrapper, and reflect off the wrapper by specular spike reflection for a polished surface or Lambertian reflection for a ground surface. The roughness of the crystal-air gap interface is set by σ_α. In this work, σ_α for both wrapping materials are 5° [24]. The PMT model is Hamamatsu R6427. The light collection performance of a positron detector is quantified by

$$LCE = \frac{N_{Det}}{N_{Gen}} \times 100\% \qquad (1)$$

where N_{Gen} is the total number of photons generated inside a scintillator, and N_{Det} denotes the number of photons detected on the photocathode of a PMT. The upper limit of LCE is around 22% owing to the QE of PMT R6427. One million ^{22}Na atoms were sampled in each simulation to suppress statistical fluctuations. The wrapping method of positron detectors is denoted by "XXX-YYY" for short, meaning that the scintillator is wrapped with material "XXX", and the long straight/L-bent light guide is wrapped with material "YYY". Material "XXX" or "YYY" can be either PTFE tape or aluminum tape.

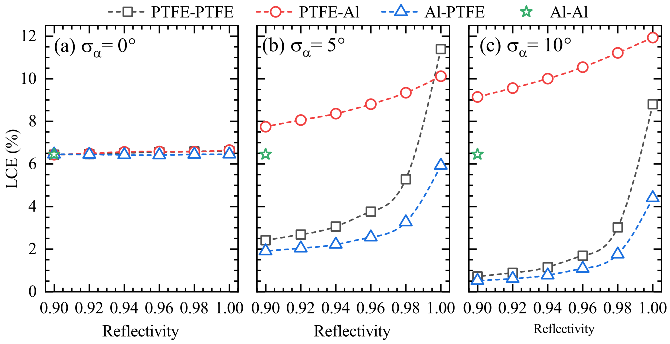

Fig. 4. The light collection efficiencies of four wrapping methods. The first material is for the scintillator, and the second is for the long straight light guide in each item. The items "PTFE-Al" and "Al-PTFE" denote hybrid wrapping methods. Optical properties are fixed for aluminum tapes ($\sigma_\alpha = 0°$, reflectivity = 0.90). The uncertainties are within 1% of the data points, which are too little to be displayed.

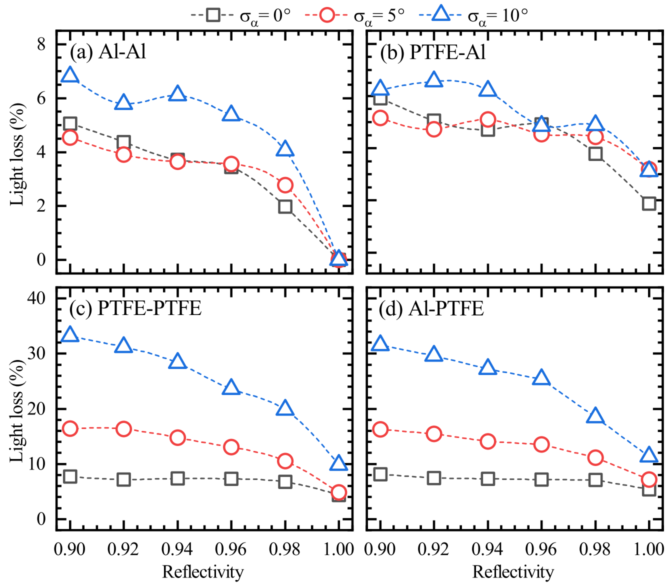

Fig. 5. Light loss of the L-bent detector compared with its straight version using the same wrapping method. The first material is for the scintillator, and the second is for the light guide in each item. Optical properties are fixed for PTFE tapes ($\sigma_\alpha = 0°$, reflectivity = 0.90) in (b) and aluminum tapes ($\sigma_\alpha = 0°$, reflectivity = 0.90) in (d). The uncertainties are within 1% of the data points, which are too little to be displayed.

III. INFLUENCES OF DETECTOR MATERIALS, SURFACE TREATMENT AND WRAPPING METHODS

A. *Impact of a long straight light guide*

As mentioned in the former section, detector materials (scintillator, light guide and wrapping materials) and their surface treatments can affect the transport of optical photons. In terms of plastic scintillators and light guides, their intrinsic optical properties cannot be changed once they are selected in an experimental project. However, the surface treatments and wrapping materials are selective, which indicates that the light collection performance can be greatly optimized with better arrangements. Before the optimization of the L-bent positron detector, a simulation study has been done to understand the influences of optical parameters on the LCE of straight detectors. The influences of wrapper reflectivity and surface roughness (σ_α) were considered in simulations.

Fig. 3 shows the LCEs of a scintillator and a long straight detector, and their ratios. Wrappers with higher reflectivity values can help achieve larger LCEs for any roughness. For single scintillators wrapped with PTFE tapes or aluminum tapes in Fig. 3(a, b), rougher surfaces can obtain higher LCEs. Comparing two wrapping materials shown in Fig. 3(c), scintillators wrapped with PTFE tapes have advantages over those with aluminum tapes in LCEs. However, surfaces with large roughness ($\sigma_\alpha = 10°$) and high reflectivity (1.0) will eliminate such advantages. The upper three graphs in Fig. 3 indicate that rougher surface treatment together with diffusive wrappers can transport more photons out of scintillators. Optical photons generated at any place inside a scintillator emit in 4π directions. The distribution width of normal facets is broader on rougher surfaces or diffusive wrapping materials. When optical photons hit the scintillator surface with more random normal facets, they are apt to reflect off to the exit surface and transmit to its coupled object (light guide or PMT). With the existence of a long straight light guide in Fig. 3(d, e), both pure wrapping methods show an over 40% decrease in LCEs with similar variation trends by comparing the data points in Fig. 3(a, b), respectively. For 100% polished surfaces ($\sigma_\alpha = 0°$), their LCEs are almost unchanged and nearly the same for both wrapping materials. For rough surfaces, LCEs for detectors wrapped with aluminum tapes are higher than those with PTFE tapes in all reflection modes as shown in Fig. 3(f). Such difference is more evident for surfaces with larger roughness and wrappers with lower reflectivity. Unlike the 4π emission of optical photons inside scintillators, photons penetrate the light guide with similar directions. Polished surface and specular wrappers have little influences on changing the direction of optical photons on the path to PMTs. From the simulation of photon behaviors in scintillators and light guides, it is possible that a novel hybrid wrapping method, "PTFE-Al", can achieve the optimal LCEs for long positron detectors. Inversely, the hybrid method, "Al-PTFE", will lead to the lowest LCEs.

To check the feasibility of hybrid wrapping methods, a specular and polished aluminum tape ($\sigma_\alpha = 0°$) with low reflectivity (0.90) was simulated by only varying the roughness and reflectivity of PTFE tapes. Fig. 4 shows the LCEs of different combinations of two wrapping materials. For perfectly polished surfaces, LCEs of four wrapping methods are nearly the same constant value. If the surface is rough, the hybrid method, "PTFE-Al", has the highest LCE and "Al-PTFE" the lowest almost in any given reflectivity. Differences between the "PTFE-Al" method and other hybrid or pure wrapping methods become bigger for rougher surfaces. It verified the conclusions drawn from Fig. 3. For "scintillator+light guide" configurations, the hybrid wrapping method - "PTFE-Al" can optimize the light collection performance to a large extent, even with imperfect surface treatment and low reflectivity wrapping materials at a lower cost.

According to the simulations and experiments on a long straight detector, it is feasible to further improve the light

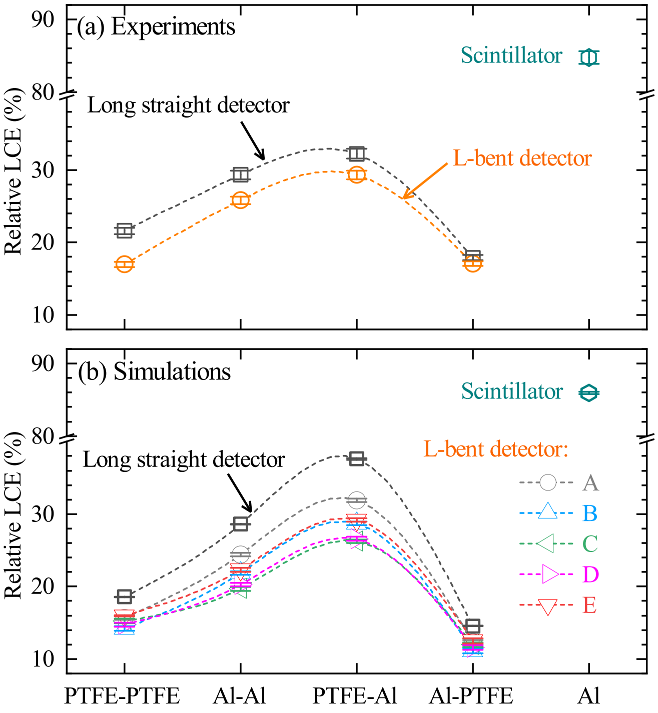

Fig. 6. Relative LCEs of positron detectors from (a) experiments and (b) Geant4 simulations. All data are relative to the scintillator wrapped with PTFE tapes. The first material is for the scintillator, and the second is for the light guide in each wrapping method. Details of bending shapes can be seen in Fig. 2. Uncertainties are within 1% of the data points, which are so small that they are displayed inside the open marks. The relative LCEs for the scintillators wrapped with PTFE tapes are 100%.

collection performance of the L-bent detector using the novel hybrid wrapping method ("PTFE-Al").

B. Impact of bending the long straight light guide with an "L" shape

After the long straight light guide is bent, the normal facets in the bent part become more complicated. As a result, light loss will occur. Simulations have been done to quantify the light loss with four different wrapping methods. The shape A in Fig. 2 was set as the bent part in Geant4. As shown in Fig. 5, variations of light loss present a dependency of wrapping materials for the bent light guide. If the light guide is wrapped with aluminum tapes, the light loss of the whole detector is no more than 7% shown in Fig. 5(a, b). It indicates that influences of the L-bent shape can be limited to a low level when wrapping the light guide with specular materials, even with relatively low reflectivity. When changing the light guide wrapping material to PTFE tapes in Fig. 5(c, d), the light losses are an order of magnitude higher than those of aluminum tapes. In terms of surface roughness, its influence on light loss is more obvious for light guides wrapped with PTFE tapes. According to these simulations, wrapping the light guide with aluminum tapes can limit the light loss induced by bending operations to a low level, even with relatively low reflectivity.

IV. EXPERIMENTAL VALIDATION AND OPTIMIZATION OF THE LIGHT COLLECTION PERFORMANCE FOR POSITRON DETECTORS

Several positron detectors were manufactured to validate the simulations and optimize their light collection efficiency under real conditions. As aluminum tapes are difficult to bend without deformations, the bent part of the L-bent detector was wrapped with PTFE tapes for both "Al-Al" and "PTFE-Al" methods. Such treatment was also considered in the simulation. The absolute LCE cannot be easily measured in experiments. Alternatively, the relative LCEs were used by comparing signal amplitudes with those of the reference detector (scintillator wrapped with PTFE tapes). Fig. 6 shows the experimental and simulation results for all detector configurations. The consistency of simulations to experiments verifies the model and parameter setups in Geant4. Owing to the limited details of optical properties for surface finish and wrapping materials set in Geant4, the simulation results deviate from the experiments by less than 5%. The experimental tests confirm that the hybrid wrapping method, "PTFE-Al", can achieve the highest LCEs for both long straight and L-bent detectors. In terms of the L-bent detector, such hybrid wrapping method increases 73% or 14% more light than the conventional pure PTFE or aluminum wrapping method, respectively. It also shows that the bending operation reduces less than 10% light with the optimal wrapping method. Fig. 6(b) shows the differences of five kinds of bending deformations. Compared to the perfectly bent detector (shape A), the absolute light losses induced by bending deformations (Shape B/C/D/E) are less than 5%, and their relative light losses are less than 20%. The symmetrically deformed shapes (B and E) have less influences than asymmetrical shapes (C and D). In terms of simulations, it is better to manufacture the detectors with perfect shapes to get the optimal LCEs. Compared the experiments with simulations, the hand-bent method more likely induces symmetrically deformation into the bent part. It is acceptable for positron counting in μSR application with a low cost (∼5 times reduction in manufacturing cost). From both experiments and simulations, the influence of bending operation and its related deformations on light loss is ignorable for μSR detection.

Compared with the single-material (only PTFE or aluminum tape) wrapping method performed at other muon facilities, the novel hybrid wrapping method (PTFE-Al) can further improve the light collection efficiency of the whole detector up to 73%. The light loss induced by the bending process can be limited within 10%.

V. DETECTOR PERFORMANCE IN THE BEAM TEST

Two optimized positron detectors (denoted as Chinese detectors) were made based on the work in section III and IV, and tested in replacement of one detector module of the EMU spectrometer [6] at ISIS Muon Facility. Pulse height spectrum measurement was conducted at first for both EMU and Chinese detectors. As shown in Fig. 7(a, d), the pulse height spectrum of the Chinese detector presents a similar "valley-peak" envelope to that of the EMU detector. Events

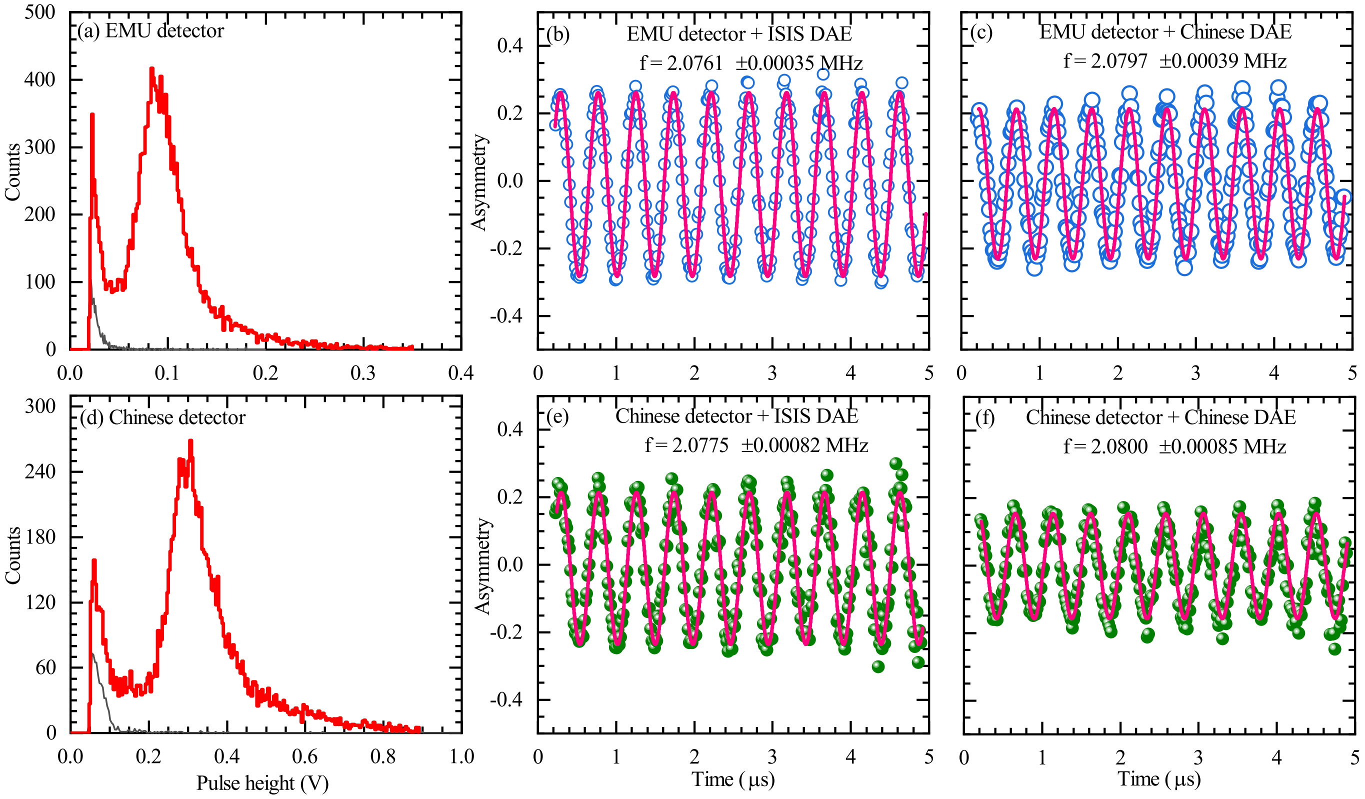

Fig. 7. (a, d) Pulse height spectra and (b, c, e, f) observable asymmetries for different detector-DAE collocations. The parameter f is the Larmor precession frequency of muon spins fitted from the oscillation of observable asymmetries. Red curves in (b, c, e, f) are fitted from the circular data points.

with amplitudes smaller than the "valley" position are composed of PMT noises and low energy positron deposition. The peak structure contributes from the energy deposition of positrons with relatively high kinetic energy. The measurement demonstrated that positrons penetrating the Chinese detector can be effectively counted. Thereafter, a transverse field (TF) measurement was done to verify if the Chinese detector can correctly detect μSR signals. Different detector-Data Acquisition Electronics (DAE) collocations were tested under a 150-G TF condition shown in Fig. 7(b, d, e, and f). Differences of covered solid angle of detectors and threshold setups in DAEs lead to the variation of asymmetry amplitude in these four panels. They can be eliminated by changing the placement of detectors and thresholds for DAEs. By comparing (e) to (b) and (f) to (c) in Fig. 7, the spin precession frequency of muons measured by the Chinese detector is almost the same as that of the EMU detector using the same DAE. Accordingly, the Chinese L-bent detector is competent for μSR applications at CSNS/EMuS.

VI. CONCLUSION

Geant4 simulations and experiments have been done to optimize the light collection performance of plastic scintillators coupled with L-bent light guides. The surface roughness, optical properties of wrapping materials and bending deformations were carefully modelled. Compared with the single-material (only PTFE or aluminum tape) wrapping method performed at other muon facilities, the newly developed hybrid wrapping method, "PTFE-Al", achieves an enhancement in light collection efficiency of 73% and 14% on the basis of merely PTFE or aluminum wrapping methods, respectively. The "L" bent shape and its deformations in the bent part have limited influences on LCE with a total percentage less than 10% using the hybrid wrapping method. The modelling of shape deformation and the selection of the optimal wrapping method provides a new guidance for the design of scintillation detectors in the μSR instrumentation or other similar application areas. Two positron detectors were manufactured based on the optimization work and tested at ISIS Muon Facility. The beam test shows that the L-bent positron detector can effectively count positrons decayed from muons, and precisely measure the muon spin behaviors inside samples. Hence that the L-bent detector design satisfies the requirement of μSR application at CSNS/EMuS, and can be mass-produced to finalize the construction of the 128-channel μSR spectrometer prototype.

ACKNOWLEDGMENT

The authors would like to thank the Muon Group and the Detector Group of ISIS Muon Facility for the technical support of μSR experiments on the EMU spectrometer.

REFERENCES

[1] F. L. Pratt *et al.*, "Magnetic and non-magnetic phases of a quantum spin liquid," *Nature*, vol. 471, no. 7340, pp. 612-616, 2011.

[2] A. D. Hillier, J. Quintanilla, B. Mazidian, J. F. Annett, and R. Cywinski, "Nonunitary Triplet Pairing in the Centrosymmetric Superconductor $\mathrm{LaNiGa_2}$," *Phys. Rev. Lett.*, vol. 109, no. 9, p. 97001, Aug. 2012.

[3] J. Perego *et al.*,"Fast motion of molecular rotors in metal–organic framework struts at very low temperatures," *Nat. Chem.*, 2020.

[4] S. J. Blundell, "Spin-polarized muons in condensed matter physics," *Contemp. Phys.*, vol. 40, no. 3, pp. 175-192, 1999.

[5] J. Tang *et al.*, "EMuS Muon Facility and Its Application in the Study of Magnetism," *Quantum Beam Sci.*, vol. 2, no. 4, p. 23, Nov. 2018, doi: 10.3390/qubs2040023.

[6] S. R. Giblin *et al.*, "Optimising a muon spectrometer for measurements at the ISIS pulsed muon source," *Nucl. Instrum. Meth. A*, vol. 751, pp. 70–78, 2014.

[7] J. S. Lord *et al.*, "Design and commissioning of a high magnetic field muon spin relaxation spectrometer at the ISIS pulsed neutron and muon source," *Rev. Sci. Instrum.*, vol. 82, no. 7, p. 73904, 2011.

[8] A. Stoykov, R. Scheuermann, K. Sedlak, J. Rodriguez, U. Greuter, and A. Amato, "High-Field μSR Instrument at PSI: Detector Solutions," *Phys. Procedia*, vol. 30, pp. 7–11, 2012, doi: https://doi.org/10.1016/j.phpro.2012.04.028.

[9] D. Tomono *et al.*, "Progress in development of new μSR spectrometer at RIKEN-RAL," in *Journal of Physics: Conference Series*, 2010, vol. 225, no. 1, p. 12056.

[10] H. K. M. Tanaka *et al.*, "Construction and performance of 128-channel segmented pulsed μSR and μe detection system at Dai Omega," *Nucl. Instrum. Meth. A*, vol. 554, no. 1–3, pp. 201–211, 2005.

[11] A. Stoykov, R. Scheuermann, K. Sedlak, T. Shiroka, and V. Zhuk, "A new detector system for the ALC spectrometer—First experience with G-APDs in μSR instrumentation," *Phys. B Condens. Matter*, vol. 404, no. 5, pp. 986–989, 2009

[12] K. M. Kojima *et al.*, "New μSR spectrometer at J-PARC MUSE based on Kalliope detectors," in *Journal of Physics: Conference Series*, 2014, vol. 551, no. 1, p. 12063.

[13] K. M. Kojima *et al.*, "Development of General Purpose μSR Spectrometer ARTEMIS at S1 Experimental Area, MLF J-PARC," in *Proceedings of the 14th International Conference on Muon Spin Rotation, Relaxation and Resonance (μSR2017)*, 2018, p. 11062.

[14] J. L. Jiang *et al.*, "Recovery Time of Silicon Photomultiplier with Epitaxial Quenching Resistors," in *Instrum.*, vol. 1, no. 1, p. 5, 2017.

[15] S. Dolinsky *et al.*, "Timing resolution performance comparison for fast and standard outputs of SensL SiPM," *2013 IEEE Nuclear Science Symposium and Medical Imaging Conference (2013 NSS/MIC),*, 2013, pp. 1-6.

[16] G. H. Eaton *et al.*, "The ISIS pulsed muon facility," in *Z. Phys. C - Part. Fields*, vol. 56, no. 1, pp. S232-S239, 1992.

[17] S. Agostinelli *et al.*, "Geant4—a simulation toolkit," *Nucl. Instrum. Meth. A*, vol. 506, no. 3, pp. 250-303, 2003.

[18] J. Allison *et al.*, "Geant4 developments and applications," *IEEE Trans. Nucl. Sci.*, vol. 53, no. 1, pp. 270-278, 2006.

[19] J. Allison *et al.*, "Recent developments in Geant4," *Nucl. Instrum. Meth. A*, vol. 835, no. 1, pp. 186-225, 2016.

[20] C. M. Poole *et al.*, "Fast tessellated solid navigation in Geant4," *IEEE Trans. Nucl. Sci.*, vol. 59, no. 4, pp. 1695-1701, 2012.

[21] J. Nilsson, V. Cuplov, M. Isaksson, "Identifying key surface parameters for optical photon transport in GEANT4/GATE simulations," *Appl. Radiat. Isot.*, vol. 103, pp. 15-24, 2015.

[22] eljentechnology.com, "GENERAL PURPOSE EJ-200, EJ-204, EJ-208, EJ-212". [Online]. Available at https://eljentechnology.com/products/plastic-scintillators/ej-200-ej-204-ej-208-ej-212. Accessed On: Mar. 24, 2021.

[23] M. Jannecek and W. M. Moses, "Optical Reflectance Measurements for Commonly Used Reflectors," *IEEE Trans. Nucl. Sci.*, vol. 55, pp. 2432-2437, 2008.

[24] E. Dietz-Laursonn, "Detailed Studies of Light Transport in Optical Components of Particle Detectors," *Aachen, Tech. Hochsch*, 2016.